Evaluating the Robustness of Ultrasound Beamforming with Deep Neural Networks

Adam Luchies and Brett Byram
Department of Biomedical Engineering
Vanderbilt University
Nashville, TN, USA
adam.c.luchies@vanderbilt.edu

***Abstract*—We evaluated the robustness of deep neural network (DNN) beamforming to noise, gross sound speed errors, and phase aberration. Training data was generated using simulations and the training data consisted of the responses from point target responses. Performance was compared to standard delay-and-sum (DAS). When the channel SNR was 10 dB, the CNR for DNN and DAS beamforming were 5.4±0.1 dB and 5.0±0.1 dB, respectively. When the channel SNR was -10 dB, the CNR for DNN and DAS beamforming were 4.1±0.3 dB and 1.9±0.1 dB, respectively. When the assumed sound speed was 10% larger than the actual sound speed, the CNR for DNN and DAS beamforming were 4.9±0.2 dB and 4.7±0.3 dB, respectively. When a near field phase screen aberration profile with FWHM of 2.5 mm and RMS of 30 ns was introduced, the CNR for DNN and DAS beamforming were 2.9±0.5 dB and 0.8±1.1 dB, respectively. Overall, these results show that DNN beamforming was more robust to the examined sources of image degradation than DAS.**

Keywords—beamforming, off-axis scattering, deep neural networks, noise, phase aberration, gross sound speed error

I. Introduction

Deep neural networks (DNNs) have been very successful in fields such as computer vision, image processing, and speech processing [1]. Previously, our group developed a model based beamforming method that suggested that DNNs might be useful for ultrasound beamforming [2, 3]. Recently, we trained DNN beamformers to improve ultrasound image quality [4]. Our results demonstrated that it was possible to train DNN beamformers using simulated ultrasound channel data and to improve *in vivo* ultrasound image quality.

In this work, we used simulation to evaluate the robustness of DNN beamformers to noise, gross sound speed error, and phase aberration. Real ultrasound scans contain these sources of degradation to certain degree and so it is important to study their effects on DNN beamforming.

II. Methods

DNN beamformers were trained to suppress off-axis scattering. FIELD II was used to simulate the responses from the combined responses of one one, two, or three scatterers [5]. The point targets were randomly located along an arc as shown in Fig. 1. The simulated array had a scanning aperture of 65 elements on transmit and receive, 70 mm transmit focal depth, 298 μm pitch, and 48 μm kerf. A Gaussian pulse with 5.208 MHz center frequency and 75% fractional bandwidth was used as the impulse response. The sampling frequency was four times the center frequency, 20.832 MHz.

The time-domain signal for a collection of scatterers was gated using window that was one pulse length long and that was centered at the transmit focus. The channel data was convereted to the frequency domain using a fast Fourier transform (FFT). DNNs were trained for a total of three frequencies, consisting of the DFT bin for the center frequency and the two adjacent DFT bins. The input to the network consisted of separted in-phase and quadrature components that were combined to form a single input vector. Fully-connected feed-forward DNNs with 130 inputs and the same number of outputs (i.e., two times the number of elements in the scanning aperture of the array) were used.

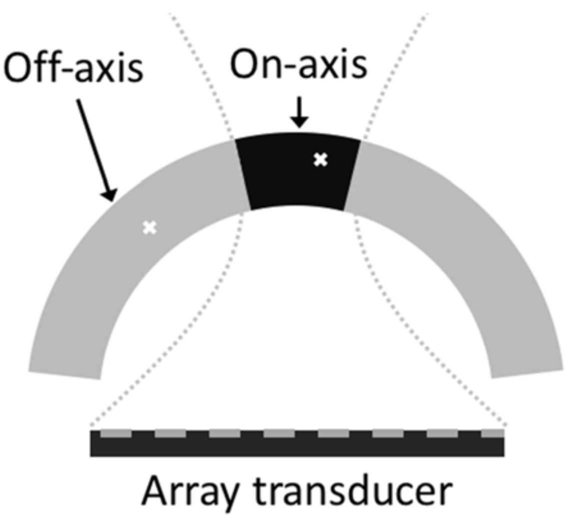

Fig. 1. One example of a two point target configuration. The combined responses of both targets was the input to the DNN and the DNN was taught to output the response from the point target in the on-axis region only.

The authors acknowledge the support of NIH R01EB020040.

Table 1 shows the hyperparameter seach space. Image quality metrics including contrast ratio (CR), contrast-to-noise ratio (CNR), and speckle SNR (SNRs) were used to evaluate the DNN beamformers.

TABLE I. HYPERPARAMETER SEARCH

Parameter	**Value**
Hidden Layers	1-5
Layer Widths	65, 130, 260, 520
Batch Size	50, 100, 500, 1000
Dropout	0, 0.1, 0.2, 0.3, 0.4, 0.5
Input Dropout	0, 0.1, 0.2
Weight Decay	0, 10^{-5}, 10^{-4}

We studied a set of 5 mm diameter simulated anechoic cysts that were at the same depth as the transmit focus. First we studied the effect of additive Gaussian noise on image quality. The channel SNR was adjusted between -10, -5, 0, 5, 10 dB.

Second, we studied the effect of gross sound speed errors on DNN beamforming. The assumed sound speed was always 1540 m/s, but the cysts were simulated using sound speeds of 1386 m/s, 1463 m/s, 1540 m/s, 1617 m/s, and 1694 m/s. Transmit focal delays were set using 1540 m/s and receive beamforming was completed using 1540 m/s.

Third, we studied the effect of phase aberration on DNN beamforming. Randomly generated aberration profiles were applied on transmit and receive to simulate the effect of a near field phase screen. The aberration profiles had full-width at half-maximum (FWHM) values of 2.5 mm and root-mean square (RMS) values of 10 ns, 20 ns, 30 ns, 40 ns.

III. Results

Fig. 2 shows the effects of electronic noise, gross sound speed error, and phase aberration on an anechoic cyst. When the channel SNR was 10 dB, the CNR for DNN and DAS beamforming were 5.4±0.1 dB and 5.0±0.1 dB, respectively. When the channel SNR was -10 dB, the CNR for DNN and DAS beamforming were 4.1±0.3 dB and 1.9±0.1 dB, respectively. When the assumed sound speed was 10% larger than the actual sound speed, the CNR for DNN and DAS beamforming were 4.9±0.2 dB and 4.7±0.3 dB, respectively. When a near field phase screen aberration profile with FWHM of 2.5 mm and RMS of 30 ns was introduced, the CNR for DNN and DAS beamforming were 2.9±0.5 dB and 0.8±1.1 dB, respectively. For the included *in vivo* scan shown in Fig. 3, the CNR for DNN and DAS beamforming were 5.0 dB and 4.3 dB, respectively.

IV. Conclusions

We evaluted the robustness of DNN beamforming to noise, gross sound speed error, and phase aberration. In general, these results show that DNN beamforming was more robust to the examined sources of image degradation than DAS.

[1] I. Goodfellow, Y. Bengio, and A. Courville, Deep Learning, MIT Press, 2016.

[2] B. Byram and M. Jakovljevic, "Ultrasonic Multipath and Beamforming Clutter Reduction: A Chirp Model Approach," IEEE Trans. Ultrason., Ferroelec., Freq. Contr., vol. 61, no. 3, pp. 428–440, 2014.

[3] B. Byram, K. Dei, J. Tierney, and D. Dumont, "A Model and Regularization Scheme for Ultrasonic Beamforming Clutter Reduction," IEEE Trans. Ultrason., Ferroelec., Freq. Contr., vol. 62, no. 11, pp. 1913–1927, 2015.

[4] A. C. Luchies and B. C. Byram, "Deep Neural Networks for Ultrasound Beamforming," IEEE Trans. on Med. Imag., vol. 37, pp. 2010–2021, 2018.

[5] J. A. Jensen and N. B. Svendsen, "Calculation of pressure fields from arbitrarily shaped, apodized, and excited ultrasound transducers," IEEE Trans. Ultrason., Ferroelec., Freq. Contr., vol. 39, pp. 262–267, 1992.

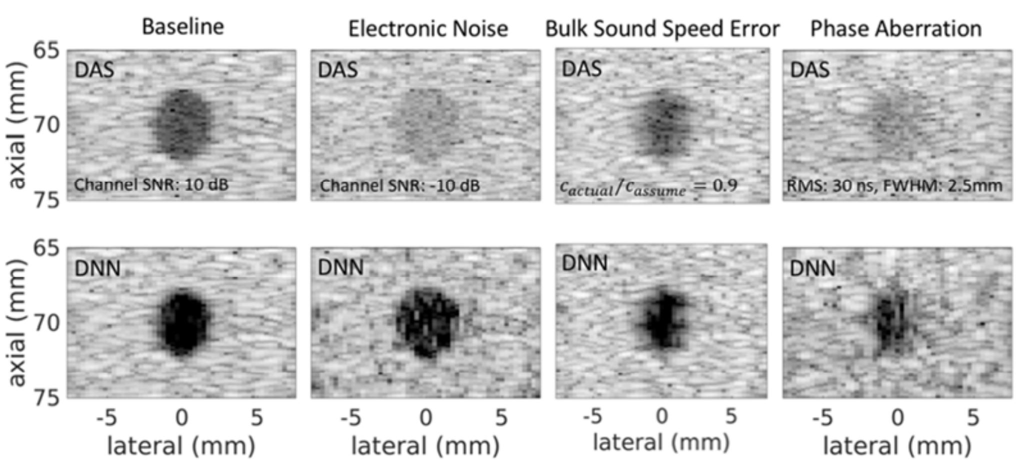

Fig. 2. Simulated anechoic cysts for DAS and DNN beamforming and with different types of image degradation.

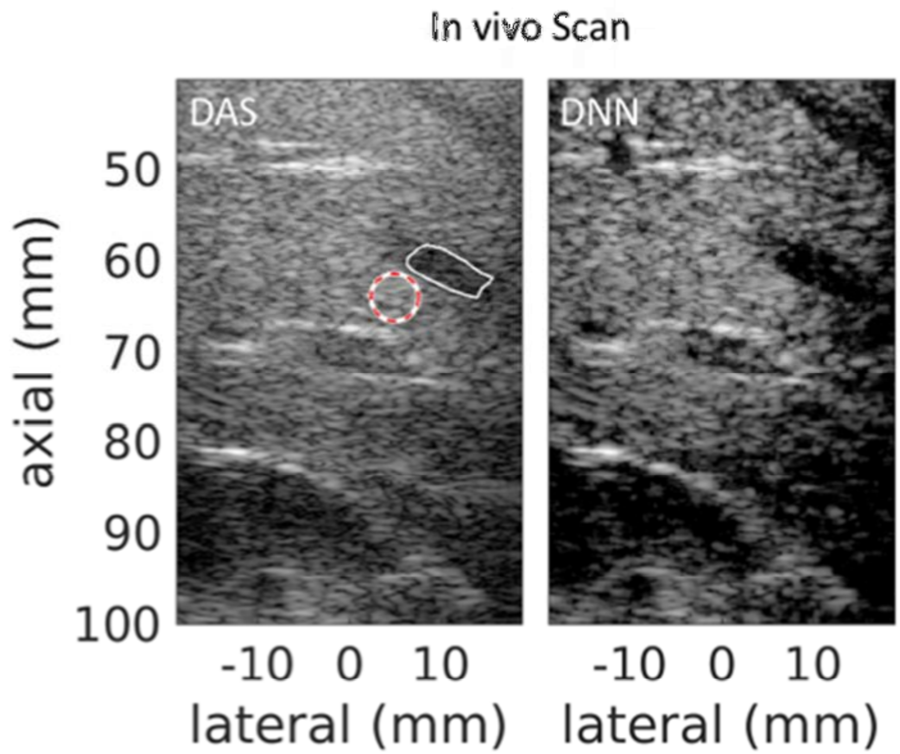

Fig. 3. *In vivo* scan of human liver.